processes

MDPI

Article

Techno-Economic Analysis of Ethylene Adsorptive Separation Using Zeolite 13X in Oxidative Coupling of Methane Integrated Process

Hamid Reza Godini [1,2,*], Nguyen Dang Huy [3], Lorenzo Ramponi [4], Nghiem Xuan Son [3], Babak Mokhtarani [5], Jens-Uwe Repke [2], Alberto Penteado [2], Giampaolo Manzolini [4], Alvaro Orjuela [6] and Fausto Gallucci [1]

[1] Inorganic Membranes and Membrane Reactors, Department of Chemical Engineering and Chemistry, Eindhoven University of Technology (TU/e), De Rondom 70, 5612 AP Eindhoven, The Netherlands; f.gallucci@tue.nl
[2] Institute of Process Dynamics and Operations, Technische Universität Berlin, Straße des 17. Juni 135, Sekr. KWT-9, D-10623 Berlin, Germany; j.repke@tu-berlin.de (J.-U.R.); albertopenteado@win.tu-berlin.de (A.P.)
[3] Department of Chemical Engineering, School of Chemistry and Life Sciences, Hanoi University of Science and Technology, Hanoi 100000, Vietnam; huy.nd174772@sis.hust.edu.vn (N.D.H.); son.nghiemxuan@hust.edu.vn (N.X.S.)
[4] Department of Energy, Politecnico di Milano, Via Lambruschini 4, 20156 Milan, Italy; lorenzo.ramponi@mail.polimi.it (L.R.); giampaolo.manzolini@polimi.it (G.M.)
[5] Chemistry and Chemical Engineering Research Center of Iran, P.O. Box 14335-186, Tehran, Iran; mokhtaranib@ccerci.ac.ir
[6] Department of Chemical and Environmental Engineering, Universidad Nacional de Colombia, Bogotá 111321, Colombia; aorjuelal@unal.edu.co
* Correspondence: h.r.godini@tue.nl or hgodini@gmail.com

Abstract: Performance analysis of the adsorptive separation of ethylene downstream of an oxidative coupling of methane (OCM) process, being an alternative process for converting methane content of natural gas or other methane-rich sources to ethylene, was studied in this research for a production capacity of 1 Mt/yr. This was motivated by observing promising adsorption characteristics and efficiency in the selective adsorption of ethylene using 13X zeolite-based sorbent. The energy and economic performance of alternative scenarios for retrofitting the adsorption unit into an integrated OCM process were analyzed. Simulations of the integrated OCM process scenarios include OCM unit, CO_2-hydrogenation, ethane dehydrogenation and methane reforming sections. The use of efficient ethylene adsorption separation enabled the improvement of the economic and energy efficiency of the integrated OCM process under specific operating conditions. For instance, the invested amount of energy and the associated energy cost per ton of ethylene in the cryogenic ethylene-purification section of the integrated process using adsorption unit are, respectively, 75% and 89% lower than the reference integrated OCM process. Under the conditions considered in this analysis, the return on investment for the final proposed integrated OCM process structure using adsorption separation was found to be less than 9 years, and the potential for further improvement was also discussed.

Keywords: adsorption; ethylene separation; oxidative coupling of methane (OCM) process; integrated process; miniplant-scale experimentation; techno-economic analysis; zeolite sorbent

Citation: Godini, H.R.; Huy, N.D.; Ramponi, L.; Son, N.X.; Mokhtarani, B.; Repke, J.-U.; Penteado, A.; Manzolini, G.; Orjuela, A.; Gallucci, F. Techno-Economic Analysis of Ethylene Adsorptive Separation Using Zeolite 13X in Oxidative Coupling of Methane Integrated Process. *Processes* **2024**, *12*, 1759. https://doi.org/10.3390/pr12081759

Academic Editors: Vincenzo Russo, Riccardo Tesser and Elio Santacesaria

Received: 28 June 2024
Revised: 4 August 2024
Accepted: 8 August 2024
Published: 20 August 2024

1. Introduction

Cryogenic separation is an energy-intensive technology commonly utilized for the downstream separation and purification of paraffins and olefins (e.g., ethylene from ethane) in industrial-scale crackers. When used for the separation of olefins in low fractions from a relatively diluted product stream, the energy efficiency of this technology is very low [1]. This is, for instance, the case for separating ethylene from the effluents of oxidative coupling of methane (OCM) reactor, which is a promising alternative process for directly converting

methane content of natural gas, biogas, or other methane-rich sources to ethylene. Alternatively, adsorption separation is a conceptually promising choice for selectively targeting the components comprising the smaller portion of the processed gas. Having considered these and after experimentally demonstrating the promising and robust adsorption separation of ethylene separation downstream of the OCM process at a miniplant-scale facility [2–4], a model-based analysis of the performance of such industrial-scale adsorption process is reported in this work. This includes a detailed simulation of the adsorption unit and an extensive model-based techno-economic analysis of an integrated OCM process with and without using the adsorption unit. Being supported by the miniplant-scale experimental data and analyzing the techno-economic performance of such an integrated process while synchronizing the main parameters in the upstream and downstream units are among the distinguished novel aspects of this study. It is also important to point out that the specifications of the reactor and the downstream units in the integrated OCM process determine not only the compositions of the feed streams to be treated by the adsorption unit but also the potential for optimal mass and heat integration between these units.

In order to assess the efficiency of the different process scenarios resulting from alternative retrofitting of the adsorption unit in the integrated OCM process, the involved units in each process scenario and their operations were simulated and analyzed. Special focus was devoted to the detailed design and simulation of the adsorption unit using the Aspen Adsorption simulator through which the impacts of the feed composition, as well as the amount of utilized sweeping gas, were assessed. In all these, a suitable type of sorbent, along with a proper set of operating conditions, should be utilized in order to secure an energy-efficient and economically attractive ethylene separation/recovery. The dimensional characteristics of the adsorption unit, including the required length and diameter of the adsorption column to secure the targeted residence time and purity, were also estimated. This was carried out by using the model-based study to be in line with the experimentally observed multicomponent breakthrough profiles. Proper detailed design of the adsorption–depressurizing–purging–desorption–pressuring cycle was also targeted using systematic model-based analysis to determine operating and structural parameters, including the required number of columns, the applied set of time steps and the switching procedure of this cycle.

Reported data from similar studies using this or other types of sorbents for the same application [3–5], for ethylene separation from different processes [6,7], or even for other olefin separation applications [8,9], were also reviewed to support the general aspects of simulating the adsorption cycle. The assumptions made in the analysis of the adsorption unit and the integration potentials of the adsorption unit within the OCM process, as well as the possible strategies for improving its performance, are also revisited through the conducted comprehensive model-based study of the industrial-scale plant. After simulating all involved units and individually validating their predicted performances, a comparative energy-economic analysis of the investigated integrated process scenarios was conducted, and its results are reported in this paper. Having conducted such a comprehensive analysis, the potential and proper utilization of the adsorptive separation of ethylene in the integrated OCM process are highlighted.

2. Conceptual Design and Demonstration of the Integrated OCM Process

The OCM reaction system consists of a surface-catalytic and gas-phase set of reactions, including the coupling of two activated methane molecules on the surface to generate ethane, which subsequently undergoes a primarily gas-phase dehydrogenation to produce ethylene. In parallel, methane and other hydrocarbons are converted to carbon oxides (mostly CO_2), hydrogen and water via undesired oxidative or reforming reactions. Therefore, at the outlet of an OCM reactor, unreacted methane, water, carbon oxides, ethylene, ethane, and a small portion of heavier hydrocarbons C_3+ (propane, propylene, etc.) are expected.

As in most oxidation processes, the net thermal balance of the OCM reactions set demonstrates a strong exothermic behavior. Having considered this and the range of temperature in which the OCM catalysts have been usually tested (>600 °C), it is clear that a special thermal-reaction engineering and reactor design is required to simultaneously control the reaction temperature and the selectivity towards the olefin. In order to control the reaction temperature, the reactive atmosphere can be diluted using an inert gas diluent such as nitrogen, steam, carbon dioxide, or extra methane using higher methane-to-oxygen ratios. Depending on the type and amount of the diluting gas, the performance of the OCM reactor and downstream units will be affected [10]. In this research, CO_2 was selected as dilution gas as it is a side product of the OCM reactions and can be selectively separated by conventional amine absorption in the downstream units and recycled back to the reactor. The excess CO_2 generated in an integrated OCM process can then be converted to value-added chemicals such as methanol via catalytic hydrogenation, and thereby, the environmental prospect and the economic performance of the whole process can be improved [11]. In such an integrated process, the generated ethane in the OCM reactor and the remaining unreacted methane will also be further converted, respectively, to ethylene and syngas via ethane dehydrogenation and methane reforming. The simulated process configuration of such an integrated process, in which the adsorption unit has been retrofitted, can be seen in Figure 1.

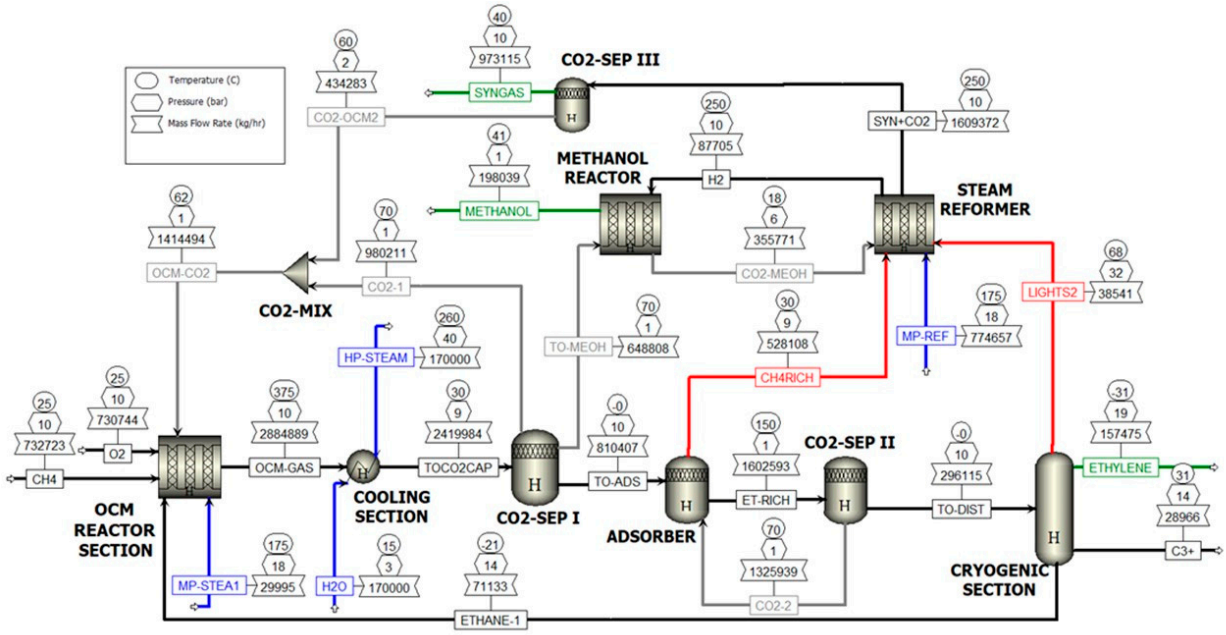

Figure 1. Simulated flowsheet of the integrated OCM process, in which the adsorption unit has been retrofitted.

In the OCM reactor section, CO_2 hydrogenation and methane reforming reactors, as well as in the downstream units, the operating conditions and the design parameters were set to secure the best performance in each section. The performance of each unit in this integrated process can be tracked through the detailed results of sequential modular simulation of the integrated process scenarios. The available experimental and industrial-scale operating data for these units indicate the plausibility of such predicted performances, especially for the adsorption section, as will be discussed in the next sections.

2.1. OCM Process Scheme

The process block-flow diagram of one possible configuration of the integrated OCM processes investigated in this research is shown in Figure 1, where connections between the main unit operations have been indicated. In such an integrated OCM process, the

potential of the high level of process integration to improve energy efficiency, as well as carbon conversion efficiency, has been highlighted. This prepares the setting to minimize the direct and indirect emission of carbon dioxide and methane. In brief, following the diagram of Figure 1, the process starts with a methane stream fed to the OCM reactor together with oxygen, recycled CO_2 for dilution and recycled ethane. The effluent of the reactor is passed through a cooling section before sending the gas to a CO_2 absorption unit (CO2-SEP I). Once most CO_2 is removed, an adsorber is used to separate C_2 hydrocarbons from methane. Alternatively, methane removal can be first accomplished, followed by CO_2 absorption removal in the CO2-SEP-II unit. CO_2 used as sweep gas is separated downstream to be recycled and reused in the adsorption unit. As previously mentioned, part of the CO_2 removed in the absorption columns is mixed in the CO2-MIX unit with the recovered CO_2 from the CO2-SEP III unit that processes the effluents of the steam reformer; the whole stream is then recycled to the OCM reactor. Another fraction of CO_2 removed in the absorption units is sent to the methanol reactor, while unconverted methane is sent to the steam reformer. Finally, C_2 hydrocarbons are fed to a distillation train operating under low temperatures (cryogenic section), where ethylene is isolated, ethane is recycled and C_3+ hydrocarbons are separated from the system.

2.2. Typical Performance of Different Units and the Experimental Observations in Miniplant-Scale

In this subsection, the design and operating specifications of the unit operations in the integrated OCM processes are described. This includes the results of the experimental analysis of the reactors, CO_2 removal, cryogenic separation of the unreacted methane and other light gases, cryogenic separation of ethane and ethylene from each other, as well as their adsorption separation from the rest of the gaseous species.

2.2.1. OCM Reactor

A packed-bed reactor was considered to represent the industrial-scale operation of the OCM reactor section. In this context, it is assumed that the catalyst is stable enough and the thermal performance of the reactor can be controlled, as has been the case for the miniplant-scale operation of the OCM reactor [12]. Mn-Na_2WO_4/SiO_2 catalyst has shown promising performance, especially in terms of securing a high C_2 selectivity under a CO_2-diluted reaction atmosphere. The selected values of methane-to-oxygen ratio (2), temperature (820 °C) and operating pressure (>5 bar) in the OCM reactor have been chosen for practical reasons. In particular, this was carried out to secure a significant amount of methane conversion and to ensure that without the need for an intermediate compression, the gas flow passes through the packed-bed reactor as well as through the following downstream units, such as absorption and adsorption units. One of the best experimentally observed reactor performances in miniplant-scale OCM operation, corresponding to a methane conversion of 45% as well as C_2 selectivity close to 60% and ethylene yield of 20% [12], was considered to represent the OCM reactor performance in this study. In fact, securing a high level of ethylene selectivity is the primary target in the conceptual design of an OCM reactor, even if it can be secured under low methane conversion. Therefore, usually even a higher concentration of unreacted methane than the one considered in this study is expected in the OCM reactor outlet. The experimentally confirmed low interaction of methane with the sorbent during the adsorption step enables relatively easier handling of the feed stream containing such a significant amount of methane and other light components [4]. This is among the main factors highlighting the promising potential of an adsorption unit to be retrofitted within an OCM process.

2.2.2. CO_2 Separation

Right after the OCM reactor, CO_2 and water should be completely removed because they are corrosive and will cause serious operational difficulties in the downstream cryogenic separation unit (e.g., freezing), even if they are present in very low concentrations. Specifically, to accommodate for using the adsorption unit, water should be completely

separated earlier, and CO_2 is preferred to be also separated, as will be discussed in detail later (in Sections 3 and 4). Conventional amine absorption technology or other well-established CO_2-separation technologies can be employed for this task [11]. However, the type of absorbing solution and the applied operating conditions should be properly chosen to avoid significant loss of ethylene and to secure an energy-efficient separation. Therefore, methyldiethanolamine absorption, under the operating pressure of 10 bar, was demonstrated to be efficient for this task in miniplant-scale operation.

2.2.3. Adsorption Unit

The mole fraction of ethylene in the product outlet stream of an OCM reactor never exceeds 10%. This highlights the selective adsorption of ethylene as the conceptually preferred separation option in this case. The targeted operating pressure in the industrial-scale OCM reactor and the CO_2-removal section could be synchronized at 10 bar which is also considered as the operating pressure in the adsorption section of the integrated process. Providing a higher operating pressure would be a straightforward technical task if needed, but it will correspond to higher compression costs. Having considered the affinity of the available sorbents towards the gas components existing in the OCM reactor outlet stream, a bed of zeolite 13X sorbent (with bulk density of 600 $kg{\cdot}m^3$, pellet radius of 3 mm, and intra-particle voidage 85%) was used in this research to establish a selective adsorption unit. Design of the adsorption/desorption columns and setting the operating conditions aim to secure a maximum recovery of ethylene along with minimum energy and fixed-capital investments. In this manner, specifically, it is targeted to minimize the ethylene loss during the adsorption step. Moreover, a well-tuned combination of pressure reduction, temperature rise and introduction of a suitable type and flow of sweeping gas enables maximizing the energy efficiency in ethylene recovery in the desorption step. Details of the simulation and validation of the predicted performance of the ethylene adsorption separation are provided in the next sections.

2.2.4. Cryogenic Separation of Ethylene, Ethane and Heavier Hydrocarbons

Cryogenic distillation can be used for the separation of ethylene and heavier hydrocarbons from lighter gases such as methane and hydrogen in the demethanizer or for the separation of ethane and ethylene (C_2) and C_3+ products from each other. This is a conventional technology and the details of its design and operation have been specified in this research based on the conducted rate-based simulation as well as the available industrial-scale operating data [1]. In this system, three distillation columns are present: (a) the demethanizer for the separation of the light gases (CH_4, H_2, and CO); (b) the C_2 splitter for the separation of ethylene from ethane and heavier hydrocarbons; (c) and the de-ethanizer column to separate ethane from heavier hydrocarbons in order to recycle it back in the EDH section. The implementation of the adsorption system aims to improve the separation of methane and light gases, mainly affecting the energy-intense operation of the demethanizer.

3. Simulation of Unit Operations

After finalizing the conceptual design of the integrated process and the specifications of its reactors and downstream units, the industrial-scale plant of this process was simulated using Aspen Plus V.11. The ethylene production capacity of the plant was specified at 1 Mt/yr, and its economic performance was evaluated using the Aspen Process Economic Analyzer (APEA). In order to precisely represent the operation of the units and their capital and operating costs, all units have been simulated considering the details of their operations. Particularly, all steps of the adsorption–desorption cycles and the rate-based simulation of the amine absorption and cryogenic distillations were simulated considering all involved phenomena and operating details. The performed techno-economic analysis enables reviewing and comparing the specifications and performance of the reference integrated OCM process with the ones in which the adsorption separation has been retrofitted.

3.1. OCM Integrated Process Scenarios Represented in Aspen Plus Supported by Experimental Data

Multi-tubular packed-bed reactor modules were used to represent all reactor sections in the integrated process structures. The experimentally observed OCM and hydrogenation reactors' performances were mapped to their industrial-scale simulated operations. In this manner, similar catalyst productivity, selectivity and conversion were considered in the experimental setups and the industrial-scale reactors while scaling up the dimensions and the processing duties proportional to the scales of the processed feed flows in different reactor scales. For the reforming and dehydrogenation reactors, the data available in the literature were similarly used as an extra validation and plausibility check. Moreover, the detailed rate-based modeling of the CO_2 absorption targeting 99.5% CO_2 removal and the cryogenic separation of the light gases (demethanizer) and heavier hydrocarbons to secure the targeted 99.9% ethylene purity have also been performed. The feed specifications and the compositions of all reactors' outlet streams, along with the typical performance of other unit operations in such integrated processes, have been reported in Figure A1.

3.2. Specifications of the Developed Aspen Adsorption Model

Having selected the sorbent (zeolite 13X) and considered the type and concentration of ethylene and other gas components in the targeted feed streams, two operating scenarios for implementing the adsorption separation were evaluated. The first one (Scenario I) is to selectively adsorb ethylene from the OCM reactor outlet after removing the water and carbon dioxide. In the second one (Scenario II), ethylene is adsorbed from the gases right after removing its water content (CO_2 rich) by cooling and condensation. In both scenarios, a hybrid combination of pressure swing adsorption (PSA) and temperature swing adsorption (TSA) is utilized to establish an energy-efficient ethylene adsorption separation.

3.2.1. Modulation of an Adsorption Column

The design and operating concept of the hybrid PSA-TSA system for each of the investigated process scenarios were simulated using the Aspen Adsorption module. The operation in the adsorption separation unit consists of four steps in a cycle, namely (1) adsorption, (2) quick depressurization-purging of the gas components in equilibrium with the saturated sorbent, (3) desorption using sweeping gas, and (4) quick pressurization using the feed stream. The full cycle was simulated through which the feeding, pressurizing, adsorption, purging, heating, desorption purging, and cooling were implemented in the Cycle Organizer of Aspen Adsorption, as schematically presented in Figure 2.

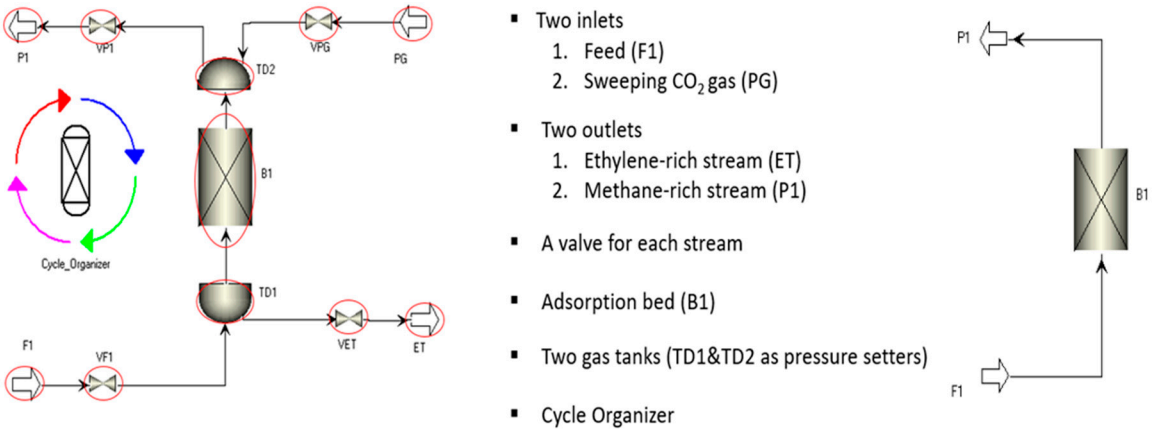

Figure 2. (**Left**): The cycle of adsorption–purging–desorption in the Aspen Adsorption simulator; (**middle**): the steps and streams involved; (**right**): the adsorber bed module.

Details of the modular representation of all steps of a typical cycle and how to implement it step-by-step in Aspen Adsorption can be found elsewhere [13]. The governing

equations as well as the involved important parameters for simulating the operation of the adsorption system in this research for all investigated scenarios, treating the CO_2-rich and CO_2-lean streams, are discussed in the following subsections.

3.2.2. Adsorption Coefficients

The adsorption coefficients (adsorption constants) represent the speed at which the molecules of an adsorbate are adsorbed at the surface of the sorbent. The adsorbed molecules accumulate at the surface and align themselves in such a way that the molecule groups with higher affinity are aligned inwards, and those with less affinity are aligned outwards. It has been reported that a linear approximation of the driving force of adsorption, calculated based on the adsorbed-phase concentration, can satisfactorily track the dynamic behavior of the adsorption phenomena. Therefore, instead of complicated, detailed modeling, which is time-consuming and requires the actual values of many parameters, linear approximation, such as the one shown in Equation (1), can be used.

$$\frac{\partial q}{\partial t} = k(q_{max} - q) \tag{1}$$

In this equation, q represents the molar concentration of the adsorbed phase per kilogram of zeolite 13X (mol·$kg_{sorbent}^{-1}$), q_{max} is the saturation concentration and k is the mass transfer coefficient (MTC) with the unit (s^{-1}). This coefficient is calculated using the data available for diffusivities, assuming that diffusion is the rate-determining step. The values of the MTC were determined based on the experimental results of miniplant-scale operation [2]. Selected sets of experimental data, in the form of breakthrough data, were introduced to the estimation mode of the Aspen Adsorption model to estimate the value of the MTC for all components so that the predicted performance matches the experimentally observed performance. Equation (2) [14] was used for estimating the values of MTCs for zeolite 13X assuming the predominant micropore diffusion (intra-crystal) step.

$$k_{mic} = \frac{15\ D_{mic}}{r_c} \qquad k_{mac} = \frac{15\ D_{mac}}{r_p} \qquad D_i = D_{i,0} e^{\frac{E_A}{RT}} \tag{2}$$

In this set of expressions, r_c is the crystal radius and r_p is the particle radius of the sorbent. D_{mic} and D_{mac} are, respectively, the micropore and macropore (intra-particle) diffusivities. The dependency of the diffusion coefficients on the temperature can be correlated using the Arrhenius equation, as shown in Equation (2). The predicted values of MTCs are listed in Table 1.

Table 1. The predicted values of the mass transfer coefficients (MTCs) for all involved components.

Components	H_2	CO	CO_2	CH_4	C_2H_4	C_2H_6	C_3H_6	C_3H_8
MTC Value	10	0.2	1×10^{-4}	0.1	1×10^{-3}	1.6×10^{-3}	7×10^{-2}	5×10^{-2}

3.2.3. Isotherms

To complete modeling the involved adsorption steps, the interaction of the diffused gas species and the surface of the sorbent is represented via isotherms. Different forms of isotherms can be utilized to calculate the equilibrium adsorption capacity of the sorbent in an adsorber model. The representative data set of isotherms in the form of a multicomponent dual-site Langmuir (DSL) model (type I), as shown in Equation (3) [15], was used in this simulation. The values of the parameters are reported in Table 2.

$$q_i = \frac{Q_{1,i} b_{1,i} p_i}{1 + \sum_{j=1}^{n} b_{1,j} p_j} + \frac{Q_{2,i} b_{2,i} p_i}{1 + \sum_{j=1}^{n} b_{2,j} p_j} \tag{3}$$

Table 2. Equilibrium data of all involved components to calculate the isotherms over Zeolite 13X [6].

Component	Q_1 [mol·kg^{-1}]	$b_{1,i}$ [Pa^{-1}]	ΔH_1 [J·mol^{-1}]	Q_2 [mol·kg^{-1}]	$b_{2,i}$ [Pa^{-1}]	ΔH_2 [J·mol^{-1}]
C_2H_4	2.91	3.14×10^{-10}	37,000	1.58	1.71×10^{-10}	30,110
C_2H_6	3.93	1.02×10^{-9}	26,500	0	0	0
C_3H_6	2.71	1.52×10^{-9}	39,820	1.14	1.25×10^{-12}	50,200
C_3H_8	2.79	7.77×10^{-10}	35,320	0.69	1.33×10^{-11}	38,000
CH_4	3.22	5.62×10^{-11}	18,290	0	0	0
H_2	7.33	1.54×10^{-9}	6947	0	0	0
CO	2.19	4.81×10^{-10}	22,445	0	0	0
CO_2	3.89	1.75×10^{-10}	58,401	3.61	2.94×10^{-5}	39,459

Here, q represents the equilibrium adsorption capacity (mmol·$g_{adsorbent}{}^{-1}$), b (bar^{-1}) is the affinity parameter, and P (bar) is the pressure. The values of the parameters in this multicomponent isotherm can be estimated by the pure gas isotherms. The temperature dependency of the Langmuir coefficients can be expressed through parameter b, which can be calculated using its reported values at different temperatures. In this manner, the isosteric heat of adsorption (ΔH) can be calculated, as shown in Equation (4) [15].

$$b_i = b_{i,0}\, e^{\frac{\Delta H}{RT}} \qquad \Delta H_i = \frac{R \ln \frac{b_i(T_1)}{b_i(T_2)}}{\frac{1}{T_1} - \frac{1}{T_2}} \tag{4}$$

Other sets of experimentally validated values of the coefficients in the DSL isotherm models for all involved species in this application could be found elsewhere [7,16,17].

3.2.4. Specifications of the Feed Gas Streams and Predicting the Breakthroughs

Operating pressure of 10 bar was considered in the adsorber which is similar to the considered operating pressure in the CO_2-removal section and the reactors. The momentum balance during the adsorption step is calculated using the semi-empirical Ergun equation, which has been demonstrated to be capable of accurately representing pressure drop in an adsorption operation [18]. The specifications of the gas stream entering the adsorber are reported in Figure A1. The feed flow, the mole fractions of each component in the feed stream and the different affinity of the sorbent towards each component will be reflected in the monitored breakthrough of the components leaving the adsorber. This is one of the main indicators for designing the duration of the adsorption cycle and the dimensions of the adsorber. In the observed breakthrough, the times at which ethane and ethylene leave the adsorber are very important. The designed residence time for the adsorber should be in the time slot between these two breakthroughs.

Initially, at t = 0 for each adsorption–purging–desorption cycle, the column is filled with mainly CO_2 at a pressure of 1.1 bar, remaining from the last cycle of the desorption step. Then, the feed is introduced and fills the column and the different components start to be adsorbed. Later, when ethane and ethylene start to leave the adsorber column, the feed is switched to the next column, and purging can be started in this column.

In order to demonstrate the validity of the simulated breakthroughs, the typical experimentally observed adsorption behavior of this system under the same set of operating conditions was simulated. The resulting predicted breakthroughs via simulation, along with the recorded experimental breakthroughs, are shown in Figure 3. Details of the miniplant-scale experimental facility utilized for testing the adsorption performance of the zeolite sorbents have been provided earlier [2].

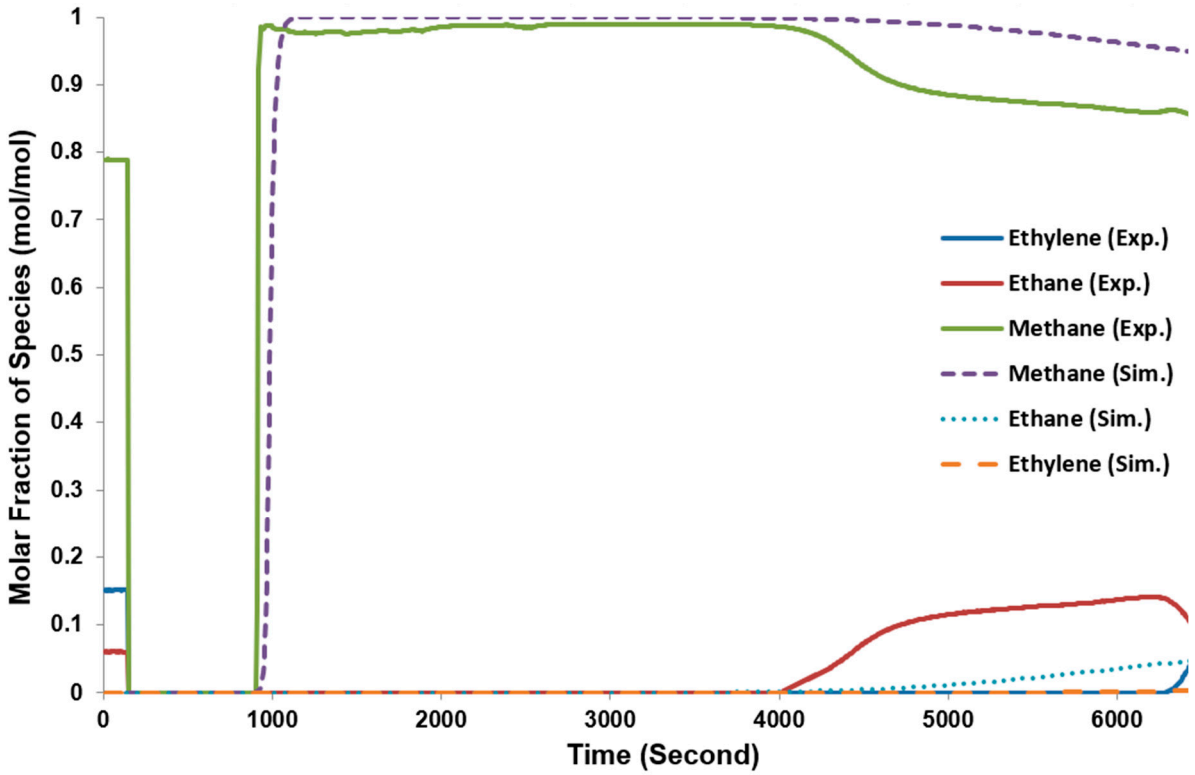

Figure 3. Predicting the breakthroughs: breakthroughs predicted by Aspen Adsorption follow similar trends as observed experimentally recorded for adsorption separation of ethylene under [T = 30 °C, flow rate of 3 lit·min^{-1}].

As seen in Figure 3, the sequence, trends and the appeared times of the simulated and experimental breakthrough time are similar. However, the slopes of some of the simulated breakthroughs are more gradual compared to their experimentally observed behaviors. The predicted gradual slope, in this case, could be attributed to the effect of numerical dispersion and can be counteracted by increasing the number of nodes used in simulation at the expense of higher computation costs. From a practical point of view, this could not affect the precision of the simulation in the conducted simulations for the techno-economic analysis because the feed is switched when ethane and ethylene start to break through, making ethylene recovery nearly 100%, no matter how stiff the slope is.

3.2.5. Design of the Adsorption Cycle

The design of the adsorption cycle in this research follows the classical steps of pressure swing adsorption in combination with the features of a temperature swing adsorption operation. Securing a minimum ethylene loss in the adsorption step and an energy-efficient removal in the desorption step, as well as the desired level of ethylene purification, are the main design criteria. Accordingly, the design and operation of the adsorption unit enabled the collection of the highest quantity of ethylene with 99.5% ethylene purity as the product stream of the C_2 splitter. The operating cost of the adsorption/desorption neutralizes a significant portion of the revenue of the products' sales. Therefore, even a slight reduction in ethylene production cannot be tolerated, so losing even 1% of ethylene would push the process to be economically infeasible. Therefore, 99% ethylene recovery was targeted in the separation.

3.2.6. Summary of the Cycle's Steps

The specifications of the integrated OCM process using the adsorption cycle simulated in Aspen Adsorption are reported in Table 3. Three parallel sets of columns are required to handle the targeted feed flow rate of 48,000 kmol/h. The designed adsorption period is

0–1300 s, which agrees with the observed experimental data [2]. The dimensions of each adsorption column are 7.5 m in diameter and 15 m in length. In the desorption period of 1300–3900 s, 5000 kmol·h^{-1} of sweep gas (CO_2) is required for each of the columns, and therefore, the overall flow rate of carbon dioxide required in this process (in all three parallel sets) is 30,000 kmol·h^{-1}. The process needs, therefore, a total of nine working adsorption columns and an additional back-up adsorption column for this processing task.

Table 3. The design specification and the considered prices.

Project's Specifications	Value	Main Cost-Factors	Value
Number of weeks per year	48	Market selling price ethylene [€/t]	900
Number of years for analysis	15	Market selling price ethane [€/t]	250
Tax rate [%/year]	10	Market selling price methanol [€/t]	220
Interested rate/Desired rate of return [%]	12	Market selling price C_3+ [€/t]	260
Economic life of project [year]	15	Market selling price HP steam [€/MJ]	0.001
Working capital percentage [%/year]	15	Market selling price methane [€/t]	110
Operating charges [%/year]	25	Market selling price oxygen [€/t]	13
Plant Overhead [%/year]	25	Cost of sorbent [€/t]	250
Salvage value [%]	10	Cost of fuel for heating [€/t]	60
Length of start-up period [week]	15	Cost of lowest cooling media $_{(-160\,^{\circ}C)}$ [€/J]	3.5×10^{-8}
Ethylene production capacity [t/year]	10^6	Cost of cooling in C_2 splitter $_{(-47\,^{\circ}C)}$ [€/t]	1.4×10^{-9}
		Cost of electricity [€/kWh]	0.05

In operating Scenario II, CO_2 was not removed before adsorption, and the feed flow rate is 85,000 kmol·h^{-1}. Consequently, five parallel sets of columns are required. Since feed gas consists of more than 40% CO_2, which is strongly adsorbed on zeolite, the bed is quickly saturated and the adsorption period lasts only 300 s for the same column size. At the end of the adsorption period, CO_2 occupies most adsorption sites making ethylene desorption faster. However, it still requires 900 s for complete ethylene recovery despite the fact that the purging flow rate is doubled. The desorption period is three times longer than the adsorption period, resulting in a total of twenty working columns and an additional back-up one. The total required CO_2 flow rate for all five sets of columns working continuously is then 150,000 kmol·h^{-1}. Scenario II is, therefore, considered inferior to Scenario I because it requires five times more CO_2 and too many adsorption columns. Hence, only Scenario I was implemented in Aspen Plus for the evaluation of the fully integrated OCM process.

3.2.7. Implementation of the Adsorption Cycles in Aspen Plus

The developed model in the Aspen Adsorption environment was implemented in Aspen Plus to be connected to the other simulated unit operations of the integrated OCM process. This enabled us to ultimately analyze its contribution to the techno-economic performance of the whole plant. The methane-rich stream leaving the adsorption column at 30 °C and 9 bar is then sent directly to the reforming section, while the ethylene-rich stream is sent to the second CO_2-removal unit before entering the cryogenic distillation section. The generated, consumed and circulated CO_2 in this integrated process has been tuned to secure the availability of the desired quantities of CO_2 dilution to the OCM reactor, the required reactant for the methanol reactor section, and the needed sweep gas for the adsorption cycles.

3.3. Economic Analysis

After implementing the units in Aspen Plus and simulating the flowsheet, the equipment was mapped into the Aspen Process Economic Analyzer (APEA), where dimensions,

construction materials and characteristics were defined. The design specifications of the plant, along with the price of the raw materials, products and utilities, have also been specified as listed in Table 3. Having considered these items, the APEA calculated the economic performance of the plant.

Details of the direct costs of the main equipment in different sections of the integrated OCM process using the adsorption unit are reported in Figure A2.

4. Process Performance Analysis

The results of the conducted techno-economic performance analysis of the integrated OCM process scenarios with and without using the adsorption unit are reported and discussed herein. Their performances are compared in terms of their energy efficiency and economic performance indicators. The contribution of each unit in separating the targeted components can be tracked by comparing the compositions of the inlet and outlet gas streams at each unit. The correspondingly calculated energy efficiency and the operating and capital costs for each unit can also be compared accordingly.

4.1. Reference Integrated Process

The specifications and the economic performance indicators of the reference integrated OCM process have been reported in Tables 3 and 4.

Table 4. A general overview of the results of economic analysis of the investigated process scenarios.

Scenarios	Reference Integrated OCM Process (Cryogenic)	Integrated OCM Process (Adsorption)
Total Capital Cost [k€]	1,076,890	1,060,147
Total Operating Cost [k€/year]	1,368,520	1,451,366
Raw Material Cost [k€/year]	734,681	726,563
Total Products Sales [k€/year]	1,900,650	1,879,500
Specific Energy per t of Ethylene in Cryogenic Section [GJ/t C_2H_4] [1]	4.2	1.1
Specific Operating Cost in Cryogenic Section [€/t C_2H_4] [1]	115	12
Total Specific Operating Cost in all Sections [€/t C_2H_4] [2]	1054	1118
Payout Period [year]	7.93	8.44

[1] These values were calculated for the direct expensive type of energy usage and the operating costs in the cryogenic section. [2] These values cover the total operating cost utilized for the production of ethylene, methanol, syngas, etc.

The data reported in Table 4 show that the operating cost in the cryogenic section of the reference integrated process is responsible for a significant portion of the total operating costs, as has also been demonstrated to be the case for the individual OCM process [10].

4.2. Performance Analysis of the Adsorption Unit for the Targeted Feed Streams

The predicted breakthroughs under the investigated designed specifications and configuration were studied and demonstrated (e.g., as shown in Figure 3) to follow similar trends as recorded experimentally. The typical composition of the gas stream exiting the adsorption column along the time, indicating the breakthrough of ethane and ethylene, can be seen in Figure 4.

As observed, the breakthrough of ethylene appears long after the breakthrough of ethane. The breakthrough of propane and propylene appears even later, and their zero-mole fraction in the adsorber outlet stream has been predicted for the whole time span shown in Figure 4. The general trends of the simulated breakthrough curve and the predicted times of appearance of the components at the adsorber outlet gas stream have been validated and found to be quantitatively and qualitatively in agreement with the experimental observations [2]. The separation performance of the adsorption unit in the

developed integrated OCM process can be highlighted by comparing the predicted mole fraction of the components in the un-adsorbed (CH_4-rich) gas stream and the desorbed (C_2H_4-rich) gas stream using sweeping CO_2, as reported in Table 5.

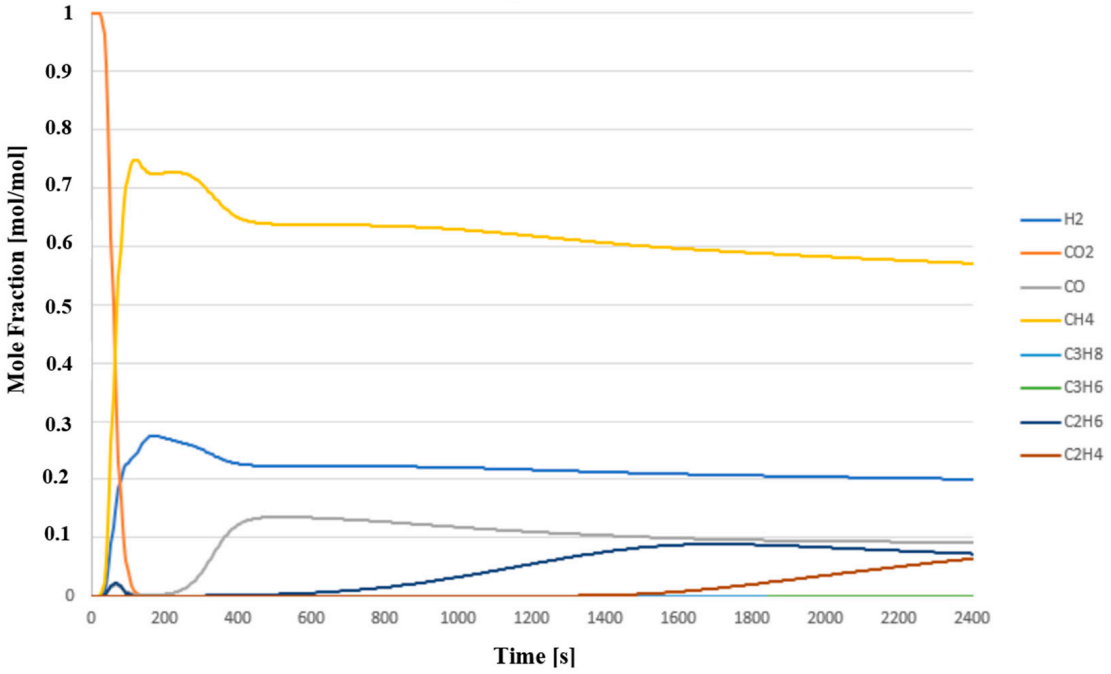

Figure 4. The breakthrough of the species targeting the ethylene adsorption separation.

Table 5. The composition of the un-adsorbed gas stream (CH_4-rich) and the desorbed (C_2H_4-rich) stream using sweep gas CO_2.

Streams	H_2 [%]	CO [%]	CO_2 [%]	CH_4 [%]	C_2H_4 [%]	C_2H_6 [%]	C_3H_6 [%]	C_3H_8 [%]
CH_4-rich	22.3	10.2	3.2	63.6	0.0	0.6	0.0	0.0
C_2H_4-rich	0.0	0.0	77.7	0.0	14.9	5.6	1.4	0.3

It is noticed that the adsorption separation significantly contributes to reducing the energy consumption in the energy-intense cryogenic section. This can be observed by comparing the specific operating cost in the cryogenic section of the integrated OCM process with and without an adsorption unit, as shown in Table 4. However, the total specific energy in the integrated OCM process using ethylene adsorption separation is higher than the one in the reference integrated process, mainly due to the significant portion of the operating cost used in separating the CO_2 sweep gas stream. In fact, this is the main factor that has resulted in poorer energy efficiency and a longer payout period of the integrated process with the adsorption separation. Nevertheless, the resulting knowledge about the expected impacts of the operating parameters on the energy-efficiency and economic performance will be instrumental in retrofitting the adsorption–separation technology to the evolving OCM technology, potentially playing a role in finalizing some of its design and operating parameters. This could be particularly impactful for securing the continual production and the targeted product's specs in relatively small-scale decentralized OCM plants.

The economic viability of this integrated OCM process using cryogenic separation, particularly for the separation of unreacted methane, is very sensitive to the exposed costs of separation [19]. Therefore, securing higher ethylene selectivity should be prioritized. This was targeted in designing the integrated process analyzed in designing this integrated process by (a) integrating the ethane dehydrogenation process to improve the overall ethylene selectivity and (b) being able to handle the consequences of using parameters

in upstream and downstream units such as using higher methane-to-oxygen ratios in the reactor and using an efficient adsorption–separation technology.

The integrated process using adsorption requires no cryogenic demethanizer, which costs 45 million Euros in the reference integrated process. In fact, the capital cost saved in this way is comparable with the additional capital cost needed for the adsorption unit. Similarly, the required compression costs of these cases are, respectively, 6 million €/year and 30 million €/year. However, the total operating costs of the integrated process using an adsorption unit is 82 million €/year higher. Reducing the cost of CO_2 removal after the desorption step can significantly reduce this. Having considered all these, it could be identified that if the ethylene loss and the operating cost of the ethylene adsorption separation or the price of the sorbent could be even slightly improved, the potential of utilizing the integrated OCM process using an adsorption unit will be further improved to the level of competing technology.

5. Conclusions

The aim of this study was to analyze the techno-economic potentials of the adsorption separation of ethylene in an integrated OCM process. This was highlighted by comparing the model-based estimated energy-efficiency and economic performance of such an integrated process with and without using an adsorption unit. The equilibrium data and the mass transfer characteristics of the 13X zeolite-based sorbent used in this study were calculated using the available experimental data to develop a detailed representative model of the adsorption operation. The adsorption unit operation was simulated in Aspen Adsorption and then integrated into the integrated OCM process simulated in the Aspen Plus simulation platform. The predicted performances of different parts of this simulated integrated process, including the reactors and downstream units, were validated using the available experimental data. In particular, the prediction and sensitivity of the developed model representing the adsorption unit were examined by tracking the breakthrough of the ethylene and ethane adsorption separation. It was found that in designing the adsorption step, recovering the maximum amount of ethylene as well as a significant portion of ethane should be prioritized. Due to the possibility of further converting ethane to highly valuable ethylene via the EDH reactor in the integrated OCM process, we can significantly enhance the economic performance of the integrated process.

The economic analysis performed on the integrated OCM process scenarios indicated that using the adsorption unit, the capital cost and operating cost of the energy-intensive cryogenic demethanizer could be completely saved. This also implies that a feed stream with higher methane-to-oxygen can be processed in an OCM reactor to secure a higher ethylene selectivity there without imposing tremendous costs in handling the unreacted methane in the process downstream. However, the total energy consumption of the integrated process in such a large-scale plant is significantly affected mainly due to the extra energy and cost needed to separate the sweep gas CO_2, composing around 80% of the processed gas. In order to possibly further reduce the operating cost of the ethylene adsorption separation, a low-interacting sweep gas such as syngas or ethane is recommended to be tested in this integrated process. In any case, tailoring the characteristics of the sorbent, particularly to reduce its affinity to adsorb the sweep gas, should also be pursued with a significant potential on the economic viability of the technology.

Moreover, a detailed desorption study should be conducted to optimize the implemented operating procedure as well as determine the amount of invested energy in different parts of the adsorption–desorption cycle. These need to be also experimentally tested to observe their technical performances as well as their impacts on reducing the operating costs. This could be particularly highlighted for improving the techno-economic prospects of the small-scale decentralized OCM plants compared to the conventional cracker technologies using cryogenic separation, in which securing the continual production and the targeted product's specs are difficult and expensive.

Author Contributions: H.R.G., conceptualization, methodology, investigation, visualization, formal analysis, validation, supervision, project administration, writing—original draft, and editing; N.D.H., methodology; investigation; visualization, formal analysis, and editing; L.R., methodology, investigation, visualization, formal analysis, and validation; N.X.S., investigation, formal analysis, validation, supervision, and editing; B.M., formal analysis, validation, and editing; J.-U.R., formal analysis and editing; A.P., formal analysis, visualization, and editing; G.M., supervision, project administration, and editing; A.O., formal analysis, visualization, and editing; F.G., formal analysis, supervision, project administration, and editing. All authors have read and agreed to the published version of the manuscript.

Funding: This research was funded by the Cluster of Excellence "Unifying Systems in Catalysis" coordinated by the Technische Universität Berlin and funded by the German Research Foundation-Deutsche Forschungsgemeinschaft, as well as the Alexander von Humboldt (AvH) foundation.

Data Availability Statement: The raw data supporting the conclusions of this article will be made available by the authors upon request.

Acknowledgments: The support provided by Daniel Salerno for conducting the Aspen simulations is greatly acknowledged.

Conflicts of Interest: The authors declare no conflicts of interest.

Nomenclature

Acronyms

APEA	Aspen Process Economic Analyzer
C_2	Ethylene and Ethane
EDH	Ethane De-Hydrogenation
MTC	Mass Transfer Coefficient
OCM	Oxidative Coupling of Methane
PSA	Pressure Swing Adsorption
TSA	Temperature Swing Adsorption

Latin alphabet

$b_{i,j}$	affinity parameter of factor *i* for specie *j*, bar^{-1}
$b_{i,0}$	standard affinity parameter of species *i*, bar^{-1}
D_i	diffusivity of species *i*, $m^2\ s^{-1}$
$D_{i,0}$	standard diffusivity of specie *i*, $m^2\ s^{-1}$
D_{mac}	Maxwell–Stefan diffusivity for macroporous diffusion, $m^2\ s^{-1}$
D_{mic}	Maxwell–Stefan diffusivity for microporous diffusion, $m^2\ s^{-1}$
E_A	Arrhenius activation energy, $J\ mol^{-1}$
k	mass transfer coefficient, s^{-1}
k_{mac}	mass transfer coefficient for macroporous diffusion, s^{-1}
k_{mic}	mass transfer coefficient for microporous diffusion, s^{-1}
p_i	partial pressure of species *i*, bar
q_i	adsorbed mole concentration of specie *i*, mol $kg_{sorbent}{}^{-1}$
$Q_{i,j}$	equilibrium mole concentration
q_{max}	adsorbed mole concentration at equilibrium of species *i*, mol $kg_{sorbent}{}^{-1}$
R	gas constant, 8.314 $J\ mol^{-1}\ K^{-1}$
r_p	radius of particle, m
r_c	radius of crystallite, m
T	absolute temperature, K
t	time, s
ΔH_i	isosteric heat of adsorption, $J\ mol^{-1}$

Appendix A

Scenario I	OCM Reactor		EDH Reactor		Cooling Section		Amine I		CO2 Hydrogenation			Adsorber		
	Inlet	Outlet	Inlet	Outlet	Inlet	Outlet	Inlet	Outlet	Inlet	To Reformer	Methanol	Inlet	Met-rich	Et-rich
Temperature [°C]	650	600	835	650	375	30	30	0	249	18	41	0	30.0	150.0
Pressure [bar]	9.89	9.79	9.99	9.98	9.78	9.46	9.46	9.71	10	6	1.4	9.71	9	1.01
Mole flow [Mmol/h]	98.5	104.7	4.0	4.2	108.9	84.7	84.7	47.9	99.3	29.4	6.2	77.3	40.6	36.9
Mole fractions														
Oxygen	0.232	Trace	0.000	0.000	0.000	0.000	0.000	0.000	0.000	0.000	0.000	0.000	0.000	0.000
Methane	0.464	0.248	Trace	0.020	0.238	0.306	0.306	0.540	Trace	Trace	0.000	0.334	0.636	Trace
Ethane	0.000	0.014	0.581	0.236	0.022	0.029	0.029	0.051	Trace	0.000	0.000	0.030	0.006	0.056
Propane	0.000	0.001	Trace	0.021	0.001	0.002	0.002	0.003	Trace	0.000	0.000	0.002	0.000	0.003
Ethylene	0.000	0.043	0.006	0.294	0.052	0.067	0.067	0.119	Trace	Trace	0.000	0.072	Trace	0.149
Propylene	0.000	0.005	Trace	0.006	0.005	0.006	0.006	0.011	Trace	Trace	0.000	0.007	0.000	0.014
Carbon Monoxide	0.000	0.040	0.000	0.002	0.038	0.049	0.049	0.087	0.044	0.109	0.000	0.054	0.102	0.000
Carbon Dioxide	0.305	0.348	0.000	0.002	0.334	0.430	0.430	Trace	0.214	0.165	0.004	0.371	0.032	0.777
Hydrogen	0.000	0.086	0.000	0.022	0.083	0.107	0.107	0.190	0.731	0.714	0.000	0.117	0.223	Trace
Water	0.000	0.212	0.413	0.398	0.206	0.004	0.004	0.000	0.007	0.003	0.001	0.014	0.000	0.000
Methanol	0.000	0.000	0000	0.000	0.000	0.000	0.000	0.000	0.004	0.009	0.995	0.000	0.000	0.000

Scenario I	Amine II		Ethylene spliter			Ethane spliter			Reformer		H2 Paladium membrane			Amine III	
	Inlet	Outlet	Inlet	Ethylene	Bottom	Inlet	C3+	Ethane	Inlet	Outlet	Inlet	H2	Syngas+CO2	Inlet	Outlet
Temperature [°C]	150.0	0	59.7	-31.0	-2.0	-2.0	31.5	-21.0	850	850	250	250	250	250	40
Pressure [bar]	1.01	9.64	20	18.9	18	18	13.97	13.95	10.2	10.1	10.08	10	10.08	10.08	9.5
Mole flow [Mmol/h]	40.9	11.2	8.2	5.5	2.7	2.7	0.67	2.1	82.8	134.2	163.7	43.5	120.2	120.2	98.0
Mole fractions															
Oxygen	0.000	0.000	0.000	0.000	0.000	0.000	0.000	0.000	0.000	0.000	0.000	0.000	0.000	0.000	0.000
Methane	Trace	Trace	Trace	Trace	Trace	Trace	0.000	0.000	0.312	Trace	0.001	0.000	0.001	0.001	0.001
Ethane	0.108	0.251	0.251	Trace	0.754	0.754	0.031	0.989	0.003	0.002	0.001	0.000	0.002	0.002	0.001
Propane	0.006	0.015	0.015	Trace	0.045	0.045	0.185	Trace	0.000	0.000	Trace	0.000	Trace	0.000	0.000
Ethylene	0.289	0.670	0.670	0.999	0.008	0.008	Trace	0.011	Trace	Trace	Trace	0.000	Trace	Trace	Trace
Propylene	0.028	0.064	0.064	Trace	0.193	0.193	0.784	Trace	0.000	0.000	Trace	0.000	Trace	0.000	0.000
Carbon Monoxide	Trace	Trace	Trace	Trace	Trace	Trace	0.000	0.000	0.050	0.192	0.177	0.000	0.241	0.241	0.295
Carbon Dioxide	0.569	Trace	Trace	Trace	Trace	Trace	Trace	Trace	0.006	0.034	0.057	0.000	0.078	0.078	0.000
Hydrogen	Trace	Trace	Trace	Trace	Trace	Trace	0.000	0.000	0.109	0.672	0.680	1.000	0.564	0.566	0.693
Water	0.000	0.000	0.000	0.000	0.000	0.000	0.000	0.000	0.519	0.099	0.081	0.000	0.111	0.111	0.007
Methanol	0.000	0.000	0.000	0.000	0.000	0.000	0.000	0.000	0.000	0.000	0.001	0.000	0.002	0.002	0.003

(**Top**)

		OCM Reactor Section					Cooling Section		CO2-Sepl				ADSORBER			
		O2	CH4	OCM-CO2	ETHANE-1	OCM-GAS	OCM-GAS	TOCO2CAP	TOCO2CAP	TO-ADS	TO-MEOH	CO2-1	TO-ADS	CO2-2	CH4-RICH	ET-RICH
Phase		Gas	Gas	Gas	Gas	Gas	Gas	Gas	Gas	Gas	Gas	Gas	Gas	Gas	Gas	Gas
Temperature	°C	25	25	60	-21	376	376	30	30	0	68	68	0	70	30	150
Pressure	bar	10.1	10.1	1.4	14.0	9.8	9.8	9.5	9.5	9.7	1.4	1.4	9.7	1.4	9.0	1.0
Mass flow	kg/hr	730744	732723	1431262	61960	2875715	2875715	2410783	2410783	801296	648827	980102	801296	1282279	614768	1506823

		CO2-SepII			Cryogenic Section				Membrane Reactor				Steam Reformer			
		ET-RICH	CO2-2	TO-DIST	TO-DIST	ETHANE-1	ETHYLENE	C3+	TO-MEOH	H2	METHANOL	CO2-MEOH	CH4-RICH	CO2-MEOH	H2	SYN+CO2
Phase		Gas	Gas	Gas	Gas	Gas	Gas	Liquid	Gas	Gas	Gas	Gas	Gas	Gas	Gas	Gas
Temperature	°C	150	70	0	0	-21	-31	32	68	250	41	18	30	18	250	250
Pressure	bar	1.0	1.4	9.6	9.6	14.0	18.9	14.0	1.4	10.0	1.4	6.0	9.0	6.0	10.0	10.1
Mass flow	kg/hr	1506823	1282279	244005	244005	61960	153806	28239	648827	87705	198040	355777	614768	355777	87705	1657497

		CO2-SepIII		
		SYN+CO2	CO2-OCM2	SYNGAS
Phase		Gas		Gas
Temperature	°C	250	60	40
Pressure	bar	10.1	1.6	9.5
Mass flow	kg/hr	1657497	451160	994296

Product	Mass Flow	Efficiency
	kg/hr	%
Ethylene	153806	21
Methanol	198040	14
C3+	28239	4
Syngas	994296	68

(**Bottom**)

Figure A1. Detailed results of simulating the integrated OCM process using an adsorption unit; (**top**): specifications of the main inlet-out streams of the processing blocks; (**bottom**): material flow rates and operating pressure and temperatures in different streams corresponding to the streams and sections represented in Figure 1.

Appendix B

	Component Name	Total Direct Cost (€)
Cooling Section	COOLING.P203	193400
	COOLING.P202	111900
	COOLING.P-201	74600
	COOLING.O2-MEM	1.30E+06
	COOLING.HX-204	244500
	COOLING.HX-203	350300
	COOLING.HX-202	350300
	COOLING.HX-201	350700
	COOLING.D-201-flash vessel	857300
Methanol Reactor	MEOH-RXN.MEOH-RXN	3.49E+06
	MEOH-RXN.MEOH-PUR-cond	1.86E+06
	MEOH-RXN.MEOH-PUR-cond acc	236800
	MEOH-RXN.MEOH-PUR-reb	736300
	MEOH-RXN.MEOH-PUR-reflux pump	109100
	MEOH-RXN.MEOH-PUR-tower	3.91E+06
	MEOH-RXN.K-402	2.31E+07
	MEOH-RXN.K-401	5.44E+07
	MEOH-RXN.HX-504	142600
	MEOH-RXN.HX-503	323500
	MEOH-RXN.HX-501	2.19E+06
	MEOH-RXN.HX-401	134500
	MEOH-RXN.D-501-flash vessel	578900
Adsorber	ADSORBER.FLASH-flash vessel	1.21E+06
	ADSORBER.FEEDHEAT	125700
	ADSORBER.CO2HEAT	1.21E+06
	ADSORBER.CO2-SET	1.03E+06
	ADSORBER.ADS-BACKUP	2.04E+06
	ADSORBER.ADS1.ADS1-3	2.04E+06
	ADSORBER.ADS1.ADS1-2	2.04E+06
	ADSORBER.ADS1.ADS1-1	2.04E+06
	ADSORBER.ADS2.ADS2-3	2.26E+06
	ADSORBER.ADS2.ADS2-2	2.04E+06
	ADSORBER.ADS2.ADS2-1	2.04E+06
	ADSORBER.ADS3.ADS3-3	2.04E+06
	ADSORBER.ADS3.ADS3-2	2.04E+06
	ADSORBER.ADS3.ADS3-1	2.04E+06
OCM Reactor	OCM.SEP102	1.16E+06
	OCM.REACT-2	3.26E+06
	OCM.OCM-REAC	3.21E+06
	OCM.K-101	6.43E+07
	OCM.HX-103	996000
	OCM.HX-102	501900
	OCM.HX-101	4.96E+06
	OCM.FURN-2	7.68E+06
	OCM.FURN-1	4.87E+07
Steam Reformer	REFORMER.RPLUG	3.28E+06
	REFORMER.MEMBRANE	3.76E+06
	REFORMER.HX703	8.46E+06
	REFORMER.HX702	2.67E+07
	REFORMER.HEAT	340000
	REFORMER.FURN-701	6.67E+07
	REFORMER.EXP	1.13E+06
	REFORMER.COMP-REF	1.70E+07
	REFORMER.COMP	3.08E+07
CO2- sep III	CO2-C3.HX-SYN	1.38E+06
	CO2-C3.FLASH-CO-flash vessel	672400
	#1#Main Tower_@T-100	4.14E+06
	#1#Main Tower @T-101	4.13E+06
	#1#Reboiler @T-101	5.12E+06
	E-101	2.82E+06
	#1#E-103	669600
	#1#E-104	1.54E+06
	#1#P-100	903200
	#1#V-101	415900

	Component Name	Total Direct Cost (€)
CO2- sep II	CO2-C2.CO2-HEAT	4.96E+06
	#1##1#Main Tower_@T-100	4.89E+06
	#2#Main Tower_@T-101	3.86E+06
	#2#Reboiler_@T-101	5.34E+06
	#1#E-101	2.40E+06
	#2#E-103	683900
	#2#E-104	1.49E+06
	#2#P-100	755900
	#2#V-101	417200
CO2- sep I	E-100	473000
	E-100-2	473000
	E-100-3	473000
	E-100-4	475100
	E-103	709200
	E-103-2	674400
	E-103-3	727000
	E-103-4	727000
	E-104	1.54E+06
	E-104-2	1.54E+06
	E-104-3	1.54E+06
	E-104-4	1.54E+06
	E-105	5.88E+06
	E-105-2	5.88E+06
	E-105-3	5.88E+06
	E-105-4	5.88E+06
	P-100	930900
	P-100-2	945600
	P-100-3	945700
	P-100-4	945700
	V-100	202200
	V-100-2	202200
	V-100-3	202200
	V-100-4	202200
	V-101	463900
	V-101-2	463900
	V-101-3	463900
	V-101-4	463900
	Main Tower_@T-100	3.30E+06
	Main Tower_@T-100-2	2.89E+06
	Main Tower_@T-100-3	2.89E+06
	Main Tower_@T-100-4	2.89E+06
	Main Tower_@T-101	4.27E+06
	Reboiler_@T-101	1.02E+07
	Main Tower_@T-101-2	4.27E+06
	Reboiler @T-101-2	1.02E+07
	Main Tower_@T-101-3	4.27E+06
	Reboiler_@T-101-3	1.02E+07
	Main Tower_@T-101-4	4.27E+06
	Reboiler_@T-101-4	1.02E+07
Cryogenic Section	ETYL-SEP.K-402	2.90E+06
	ETYL-SEP.K-401	3.22E+06
	ETYL-SEP.HX	241600
	ETYL-SEP.HEAT	1.65E+06
	ETYL-SEP.ETHL-SEP-cond	904500
	ETYL-SEP.ETHL-SEP-cond acc	583000
	ETYL-SEP.ETHL-SEP-reb	357500
	ETYL-SEP.ETHL-SEP-reflux pump	249800
	ETYL-SEP.ETHL-SEP-tower	8.09E+06
	ETYL-SEP.ETHA-SEP-cond	129000
	ETYL-SEP.ETHA-SEP-cond acc	210600
	ETYL-SEP.ETHA-SEP-reb	159700
	ETYL-SEP.ETHA-SEP-reflux pump	74600
	ETYL-SEP.ETHA-SEP-tower	1.00E+06

Component Name	Total Direct Cost (€)
Cooling Section	3833400
Methanol Reactor	91155200
Adsorber	12249000
OCM Reactor	134815400
Steam Reformer	158211500
CO_2-Separation Section	135541100
Cryogenic Section	19775300

Figure A2. Detailed results of the performed economic analysis of the integrated OCM process using adsorption unit: direct costs of the main equipment in different sections.

References

1. Avendaño, S.J.; Pinzón, J.S.; Orjuela, A. Comparative assessment of different intensified distillation schemes for the downstream separation in the oxidative coupling of methane (OCM) process. *Chem. Eng. Process. Process Intensif.* **2020**, *158*, 108172. [CrossRef]
2. Mokhtarani, B.; Repke, J.-U.; Son, N.X.; Wozny, G.; Yilmaz, N.M.; Senturk, K.; Godini, H.R. Miniplant-Scale Demonstration of Ethylene Adsorption Separation in Downstream of an Oxidative Coupling of Methane Process. *Ind. Eng. Chem. Res.* **2021**, *60*, 11778–11788. [CrossRef]
3. Bachman, J.E.; Reed, D.A.; Kapelewski, M.T.; Chachra, G.; Jonnavittula, D.; Radaelli, G.; Long, J.R. Enabling alternative ethylene production through its selective adsorption in the metal–organic framework Mn_2(m-dobdc). *Energy Environ. Sci.* **2018**, *11*, 2423–2431. [CrossRef]
4. García, L.; Poveda, Y.A.; Rodríguez, G.; Esche, E.; Godini, H.R.; Wozny, G.; Repke, J.-U.; Orjuela, A. Adsorption separation of oxidative coupling of methane effluent gases. miniplant scale experiments and modeling. *J. Nat. Gas Sci. Eng.* **2019**, *61*, 106–118. [CrossRef]
5. Golipour, H.; Mokhtarani, B.; Mafi, M.; Moradi, A.; Godini, H.R. Experimental measurement for adsorption of ethylene and ethane gases on copper-exchanged zeolites 13X and 5A. *J. Chem. Eng. Data* **2020**, *65*, 3920. [CrossRef]
6. van Zandvoort, I.; van der Waal, J.K.; Ras, E.-J.; de Graaf, R.; Krishna, R. Highlighting non-idealities in C_2H_4/CO_2 mixture adsorption in 5A zeolite. *Sep. Purif. Technol.* **2019**, *227*, 115730. [CrossRef]
7. Golipour, H.; Mokhtarani, B.; Mafi, M.; Khadivi, M.; Godini, H.R. Systematic Measurements of CH_4 and CO_2 Adsorption Isotherms on Cation-Exchanged Zeolites 13X. *J. Chem. Eng. Data* **2019**, *64*, 4412. [CrossRef]
8. Narin, G.; Martins, V.F.D.; Campo, M.; Ribeiro, A.M.; Ferreira, A.; Santos, J.C.; Schumann, K.; Rodrigues, A.E. Light olefins/paraffins separation with 13X zeolite binderless beads. *Sep. Purif. Technol.* **2014**, *133*, 452–475. [CrossRef]
9. Khalighi, M.; Karimi, I.A.; Farooq, S. Comparing SiCHA and 4A zeolite for propylene/propane separation using a surrogate-based simulation/optimization approach. *Ind. Eng. Chem. Res.* **2014**, *53*, 16973–16983. [CrossRef]
10. Godini, H.R.; Azadi, M.; Penteado, A.; Khadivi, M.; Wozny, G.; Repke, J.-U. A multi-perspectives analysis of methane oxidative coupling process based on miniplant-scale experimental data. *Chem. Eng. Res. Des.* **2019**, *151*, 56–69. [CrossRef]
11. Godini, H.R.; Azadi, M.; Khadivi, M.; Schomäcker, R.; Gallucci, F.; Wozny, G.; Repke, J.-U. Multi-Scale Analysis of Integrated C_1 (CH_4 and CO_2) Utilization Catalytic Processes: Impacts of Catalysts Characteristics up to Industrial-Scale Process Flowsheeting, Part II: Techno-Economic Analysis of Integrated C_1 Utilization Process Scenarios. *Catalysts* **2020**, *10*, 488. [CrossRef]
12. Godini, H.R.; Gili, A.; Görke, O.; Simon, U.; Hou, K.; Wozny, G. Performance analysis of a porous packed-bed membrane reactor for Oxidative Coupling of Methane: Structural and operational characteristics. *Energy Fuels* **2014**, *28*, 877–890. [CrossRef]
13. Wood, K.R.; Liu, Y.A.; Yu, Y. *Design, Simulation and Optimization of Adsorptive and Chromatographic Separations: A Hands-On Approach*; Chapter 1: Simulation of Adsorption Processes; Wiley-VCH Verlag GmbH & Co. KgaA: Hoboken, NJ, USA, 2018; ISBN 9783527344697 (Print)/9783527815029 (Online). [CrossRef]
14. Garg, D.; Ruthven, D. Linear Driving Force Approximations for Diffusion Controlled Adsorption in Molecular Sieve Columns. *AIChE J.* **1975**, *21*, 200–202. [CrossRef]
15. Butt, H.; Graf, K.; Kappl, M. *Physics and Chemistry of Interfaces*; Wiley: Hoboken, NJ, USA, 2003; pp. 177–205.
16. Cavenati, S.; Grande, C.A.; Rodrigues, A.E. Adsorption equilibrium of Methane, Carbon Dioxide and Nitrogen on Zeolite 13X at High Pressures. *J. Chem. Eng. Data* **2004**, *49*, 1095–1101. [CrossRef]
17. Brea, P.; Delgado, J.A.; Agueda, V.I.; Gutierrez, P.; Uguina, M.A. Multicomponent adsorption of H_2, CH_4, CO and CO_2 in zeolites NaX, CaX and MgX. Evaluation of performance in PSA cycles for hydrogen purification. *Microporous Mesoporous Mater.* **2019**, *286*, 187–198. [CrossRef]
18. Sereno, C.; Rodrigues, A. Can steady-state momentum equations be used in modelling pressurization of adsorption beds? *Gas Sep. Purif.* **1993**, *7*, 167–174. [CrossRef]
19. Nghiem, X. Ethylene Production by Oxidative Coupling of Methane: New Process Flow Diagram Based on Adsorptive Separation. Ph.D. Thesis, Technical University of Berlin, Berlin, Germany, 2014.